# Comparative evaluation of eight legislated driving schedules in terms of cycle metrics and emissions from a diesel-powered turbocharged van

**Evangelos G. Giakoumis* and Alexandros T. Zachiotis**

Internal Combustion Engines Laboratory, School of Mechanical Engineering, National Technical University of Athens, Greece

***** Corresponding author. Email address: vgiakms@central.ntua.gr (E. Giakoumis)

## ABSTRACT

The present work compares, on a fundamental basis, the performance and emissions of a diesel-engined large van running on eight legislated driving cycles, namely the European NEDC, the U.S. FTP-75, HFET, US06, LA-92 and NYCC, the Japanese JC08 and the Worldwide WLTC 3-2. It aims to identify differences and similarities between various influential driving cycles valid in the world, and correlate important cycle metrics with vehicle exhaust emissions. The results derive from a computational code based on an engine mapping approach, with experimentally derived correction coefficients applied to account for transient discrepancies; the code is coupled to a comprehensive vehicle model. Soot as well as nitrogen monoxide are the examined pollutants. Only the driving cycle schedule is under investigation in this work, and not the whole test procedure, in order to identify vehicle speed (transient) effects of the individual cycles only. The recently developed WLTC 3-2 is the cycle with a very broad and at the same time dense coverage of the vehicle's/engine's operating activity, being thus particularly representative of 'average' real-world driving. Even broader is the distribution of the US06, whereas particularly thin and narrow that of the modal NEDC. It is also revealed that the more transient cycles, e.g. the NYCC or the US06, are also the ones with the highest amount of engine-out pollutant emissions and energy consumption. Relative positive acceleration and stops per km are

found to correlate very well with energy and fuel consumption and all emitted pollutants.

***Keywords*****:** Driving cycle; Nitrogen oxides; Relative positive acceleration; Soot; Transient operation; Turbocharged diesel engine

## 1. Introduction

For many decades, the certification procedure for new light-duty (LD) vehicles has been accomplished applying a driving cycle procedure. The first test cycles, along with the relevant emission limits, were legislated in the late 60s, and initially concerned (gasoline) passenger cars and later light-duty trucks/vans. The pioneering regions were California (California 7-mode cycle valid from 1966 in California, and from 1968 in the rest of the United States, up to 1971), and Japan (4-mode or J4 cycle, valid from 1966 to 1972) (Degobert, 1995; Berg, 2003; Giakoumis, 2017). Europe followed in 1970, as did, in the following decades, many other areas of the world such as China, India, Australia, Canada, South Korea, and South America (transportpolicy.net).

By employing a driving cycle for the certification of new vehicles, on the one hand a broad range of the engine's speed and torque is under test, and, on the other, its transient behavior. Certification cycles are characterized by relatively long duration (typically 20–30 min), and comprise various speed and load changes, cold and/or hot starting, and sometimes motorway driving as well. Applying a driving cycle for the certification of new vehicles means that simulation of the most frequent daily driving (transient) conditions is encompassed in the certification procedure (Giakoumis, 2017).

Over the last decades, there has been a huge amount of research articles and projects investigating driving cycle effects on performance and mostly exhaust emissions from light-duty vehicles (e.g. Andre et al, 1994; Joumard et al., 2000; Filipi et al., 2001; Pelkmans and Debal, 2006; Tzirakis et al., 2006; Sileghem et al., 2014; Bielaczyc et al., 2015; Marotta et al., 2015; Dimaratos et al., 2016). In the vast majority of these research efforts, experimental facilities suited to driving cycle measurement and experimentation were used.

Owing to the substantial cost involved in experimenting on a variety of test cycles, the object of research was usually the study of emissions on one or two, and only rarely more than a few cycles, although often more than one vehicles were studied.

The scope of the present work is to expand on the previous analyses by comparing a large number of legislated driving cycles with respect to vehicle and engine performance and exhaust emissions; this will be accomplished on a fundamental basis with the emphasis on the engine behavior and performance. The aim is to identify similarities and differences between the various driving schedules, and correlate them with important cycle metrics. More specifically, eight light-duty vehicles drive cycles will be studied, namely: a) the European NEDC, b) the U.S. federal FTP-75, c) the U.S. federal highway HFET, d) the U.S. supplemental US06, e) the California LA-92, f) the New York City cycle (NYCC), g) the Japanese JC08, and h) the worldwide WLTC 3-2. With the exception of the NYCC, all the other cycles are used (or intended to be used) for tailpipe emission certification of new light-duty vehicles such as passenger cars and light-duty trucks. To the best of the authors' knowledge, no such extended comparative analysis of legislated driving cycles has ever been performed, covering European, American, Japanese and Worldwide drive schedules.

Unlike the previously mentioned approaches, however, the current analysis is not purely experimental but rather combines "simulation" and experiment, being thus considerably less costly. It is also easily applicable when the purpose is to identify differences between various driving schedules on a fundamental basis, as is the object of the present work. More specifically, it is based on a steady-state experimental mapping of the engine in hand applying suitable correction coefficients to account for the significant discrepancies encountered during transients (detailed in Section 3). These coefficients have been derived from discrete accelerations, such as the ones experienced during a driving cycle. The emissions estimation is combined with a comprehensive vehicle model that 'runs' each time on the requested test schedule (Giakoumis and Lioutas, 2010).

The analysis presented in the next sections is two-fold. Firstly, a comparison of fundamental important cycle metrics will be presented in

Section 2 for the eight examined driving schedules. Afterwards, the engine/vehicle performance and engine-out emissions from the vehicle model will be investigated in Section 4. The results presented correspond to a large diesel-powered van belonging to category $N_1$ Class III according to European regulations. For the current study, the examined emissions are soot, nitrogen monoxide (NO) and carbon dioxide ($CO_2$).

It is highlighted that in the analysis that follows: a) all emitted pollutants discussed are engine-out and concern hot-started operation only (fully warmed-up engine conditions from the beginning of each cycle), and b) only the vehicle speed schedule of the cycles is under test and not the whole procedure, as the aim is to identify cycle differences located in the driving schedule only.

## 2. Brief historical overview, and comparison of the main attributes of the examined driving cycles

In Europe, the first driving cycle was introduced in 1970 (Directive 70/220/EEC). This was a modal, 'repetitive' cycle (a single 185-s 'ECE-15' schedule run four times), exclusively urban oriented, known as UDC – Urban Driving Cycle. In 1992 (Euro 1 emission standard), a motorway segment, of modal kind too, was added, the extra-urban driving cycle or EUDC (Directive 91/441/EEC); beginning with the Euro 3 emission standard in 2000, the entire cycle has been known as the New European Driving Cycle or NEDC (Directive 98/69/EC). In general, the NEDC, illustrated in Fig. 1, is quite simple to drive and thus easily repeatable. However, it does not account for real driving behavior in actual traffic, containing many constant-speed and constant-acceleration parts. In fact, from several observations it has been shown that in Europe the gap between fuel consumption and emissions experienced by the vehicle on the road and those measured at type approval is higher compared to other areas of the world (summarized in Giakoumis, 2017). The overall simplistic pattern of the NEDC, and the exact gear-shift schedule, make it easy for the manufacturers to implement cycle beating techniques. Moreover, since it is run only once, cold started, its short distance

might over-emphasize cold-starting emission effects. Oddly for its outdated structure, maximum speed is relatively high, at least compared to its Japanese (JC08 and earlier J10-15) and U.S. (FTP-75 and HFET) counterparts.

Owing to the simplified and ‘stylized’ form of the NEDC, the European authorities, even with considerable delay, have decided to adopt a true transient cycle from September 2017. This is going to be the worldwide harmonized light-duty vehicles test cycle, WLTC, together with the corresponding test procedure WLTP (GTR No.15, 2014). The WLTC is a suite of cycles, constructed based on measurements from many countries in the world (Europe, USA, Japan, S. Korea and India), with different speed/time schedules depending on the tested vehicle’s power to mass ratio (PMR); the corresponding speed/time trace of Class 3-2 or 3b (under investigation in the present work), which is suitable to the majority of European cars, is demonstrated in Fig. 1. The WLTC, compared to the NEDC, lasts longer and covers more than double distance (see Table 1 that compares some important technical attributes of the cycles). This is then reflected into cold-start emission effects being relatively lower. From a measurement point of view, the longer duration of the WLTC poses a burden on the test-bed capacity (e.g., sampling bags). Furthermore, the WLTC has higher maximum, average and driving speeds, and almost half the idling period.

The JC08, also illustrated in Fig. 1, is the current certification cycle for light-duty vehicles in Japan, having replaced the earlier, modal J10-15 and J11 cycles employed for almost 30 years. The JC08 is a truly transient cycle but, as confirmed in Fig. 1, the focus is to a large extent on congested-city traffic conditions. The idle period is long, the vehicle speeds relatively low, and the motorway part rather underestimated. This cycle exhibits the longest single stop phase (76 s) from all cycles investigated in this study. For certification purposes, the JC08 is run twice, ‘hot’ and ‘cold’, with 75–25% weighting factors respectively (transportpolicy.net; Giakoumis, 2017).

Contrary to Europe and Japan, where the ‘best cycle’ procedure is followed, in the United States a multiple-certification cycle approach is employed. At the moment, four different cycles are used during each light-duty vehicle’s certification test (regarding tailpipe emissions), namely the

FTP-75, the HFET, the supplemental US06 and the supplemental SC03. The FTP-75 (Fig. 1), developed during the late 60s (Kruse and Huls, 1973), is the ‘base’ cycle, simulating mostly urban driving conditions. The cycle has a real transient pattern, and covers a relatively wide range of driving conditions; however, it is based on data from a single vehicle from the late 60s. It is run ‘cold’ but also incorporates a hot-started segment after a 10-min engine shut-down. Unarguably, it is not complete in terms of both achieved vehicle speeds and accelerations. Oddly, its limited-duration high-speed segment is at the beginning, a fact that influences decisively the engine and after-treatment systems’ thermal status. As a result, it cannot be considered fully representative, therefore it is supplemented in the United States by three additional cycles that address its shortcomings, the HFET, US06 and SC03. Collectively, these four cycles constitute a very good mix of daily driving activity (Giakoumis, 2017), as will be discussed in Section 4.

More specifically, the HFET (highway fuel economy test) simulates interstate highway and rural driving conditions, and is employed primarily for fuel economy calculations. It was developed in the early 70s using the chase-car approach, in regions were a strict 55-mph limit was valid (Kruse and Paulsell, 1974); hence, the rather low, for today standards, maximum speeds. The supplemental US06, developed in the early 90s from measurements conducted mainly in Baltimore and Los Angeles, addresses the need for more aggressive driving that is absent in the FTP-75 (U.S. EPA, 1993). The speed schedules of both cycles are illustrated in Fig. 1 (the supplemental SC03, which addresses the need to test the vehicle with the air condition on, is not included in the current investigation).

Further to the above, the California LA-92, developed in the early 90s, forms part of the upcoming U.S. Tier 3 emission certification, being the supplemental test cycle for Class 3 HDVs (gross vehicle weight rating/GVWR 10–14,000 lbs) that are chassis tested. Like the FTP-75, it comprises three parts illustrated in Fig. 1, namely a 300-s cold-started phase, a 1135-s stabilization phase, and, after a 10-min engine shutdown, the initial 300-s phase, this time run hot-started (Austin et al., 1993).

The last investigated U.S. cycle is the New York City cycle (NYCC). This driving schedule was developed in the mid-70s, and was initially employed in

various research projects for (sulfate) emission testing. Following the Clean Air Act Amendments of 1990, Section 202(k), the cycle forms in the U.S. certification program a component of the hydrocarbon (HC) evaporative emissions running losses test (Giakoumis, 2017). The NYCC has been included in the present investigation as an example of an ‘extreme’ cycle with stop-and-go congested driving conditions.

The main technical specifications of the eight driving schedules are summarized in Table 1. More data, including detailed historical background on the cycles’ development, is available in (Giakoumis, 2017). The following remarks can be made with reference to Table 1.

– Both the U.S. FTP-75 and the WLTC Class 3-2 have the longest duration (31 and 30 min respectively), followed by the California LA-92 (approx. 29 min for the whole, three-bag run shown in Fig. 1). This also leads to these cycles exhibiting the longest distance traveled, over 17.5 km.

– On the other hand, the US06, as well as the NYCC, have the shortest duration (10 min). Owing to much higher speeds and shorter idling period, the distance covered during the US06 is more than 6 times that during the urban NYCC.

– The NYCC is the most extreme cycle. It covers the shortest distance (lower than 2 km), has the lowest average speed (approx. 11 km/h) and the longest idling period (32%) – all indicative of cycles simulating exclusively congested urban driving.

– The Japanese JC08 –as did its predecessor the J10-15– exhibits an idling period of approximately 29%, indicative of the heavily congested traffic conditions in a big Japanese city. It has rather low maximum and average speeds, in contrast to the European NEDC and the WLTC, as driving habits are much different in Japan compared to Europe.

– In contrast to the NYCC and JC08, the US06 and HFET manifest the shortest idling period, hence longest duration of driving time, as well as the highest values of average vehicle speed; this is not surprising since both cycles simulate (primarily) highway driving. The third ranking cycle in this regard is the WLTC 3-2, followed closely by the California LA-92.

– The European NEDC is the only modal cycle (all the other are true transient schedules derived from actual measurements on the road), and

shows the lowest maximum acceleration. One of its unique features is the very long cruising period (39%), not compatible with the daily driving experience.

– On the contrary, three U.S. cycles, the NYCC, US06 and California LA-92 have the maximum number of accelerations/min, maximum acceleration and maximum average acceleration; characteristics that strongly affect the amount of (engine-out) emissions particularly from turbocharged vehicles (Watson and Janota, 1982; Benajes et al., 2002; Rakopoulos and Giakoumis, 2009).

– Relative positive acceleration (RPA) is highest for the mostly transient, exclusively urban NYCC, and lowest for the exclusively motorway HFET. Particularly low is the value of RPA for the NEDC.

As evidenced from the data in Table 1 and the speed-time traces of Fig. 1, LD driving cycles differ considerably between themselves, in terms of average and maximum speeds, duration, covered distance, harshness and representativeness of real driving activity, particularly so when they originate from different regions in the world.

## 3. Methodology

The methodology employed for the estimation of performance and emissions during the driving cycles has been detailed in previous publications, including one in this very Journal (Giakoumis and Alafouzos, 2010; Giakoumis and Lioutas, 2010; Gakoumis and Zachiotis, 2017); only a brief description is provided here, for the sake of completeness, with reference to Fig. 2. As was the case with the relatively few similar mapping-based approaches developed in the past (e.g. Rackmil et al. 1988; Jiang and van Gerpen, 1992; Ericson et al., 2005; Bishop et al., 2015; Zhou and Jin, 2017), the context of quasi-linear modeling (Gambarotta et al., 2001) is, in general, followed.

Initially, a detailed experimental investigation of the engine was performed at steady-state conditions to derive its mapping with regard to performance and emissions. For the current investigation, the engine parameters under consideration were nitric oxide (NO), soot and fueling (hence $CO_2$ emissions).

NO and soot emissions were chosen owing to the fact that a detailed set of experimental measurements for these two pollutants was available under both steady-state and transient conditions. NO was considered since it forms the biggest part of $NO_x$ emissions from diesel engines, whereas soot is studied here as a surrogate to particulate matter, which is very difficult to measure instantaneously.

Based on the initial measurements at steady-state conditions, a quasi-steady mapping of the engine performance and (engine-out) emissions was initially accomplished. More specifically, for each engine rotational speed, a $4^{th}$ order polynomial was formulated for every interesting property with respect to the engine torque (Giakoumis and Lioutas, 2010).

Afterwards, a variety of transient schedules was conducted, using fast-response soot and NO analyzers. The transient schedules investigated were discrete accelerations at various loads, such as the ones experienced during a cycle, from a variety of initial engine speeds and for a variety of demanded speed changes. By doing so, we were able to assess the emission overshoot experienced by the current engine during transients, a very essential element when turbocharged engines are operated (Watson and Janota, 1982; Benajes et al., 2002). From the engine experimentation during transients, correction coefficients were derived for each pollutant that were used to 'correct' (i.e. increase) the steady-state emissions (Giakoumis and Zachiotis, 2017). Based on the block diagram of Fig. 2, at each 'second' in the cycle:

- From the vehicle speed, the actual engine speed and torque are calculated based on a drive-train model for the vehicle concerned (Winterbone et al., 1977; Gillespie, 1992). The vehicle model employed in this work is quite advanced, incorporating, among other things, the effect of the equivalent rotating masses' inertia (engine, driveshaft, wheels), tire slip effects, different gear-shift strategies etc.
- an interpolation is performed from the digitized engine map to assess the corresponding *steady-state* emissions and fueling/$CO_2$ at the exact engine speed and load operating point.
- correction coefficients are subsequently applied to the steady-state emissions of the previous step in order to evaluate the 'real' *transient*

emissions; these coefficients, evaluated after extensive transient experimentation on the engine in hand, are based on the specific transient condition (speed and/or load increase) experienced by the engine.

Finally, integration of the instantaneous results is performed over the whole cycle providing the overall emissions and fuel consumption/$CO_2$.

Table 2 provides the main technical characteristics of the engine under study; furthermore, it provides data for a typical (hypothetical) vehicle the engine is installed in, needed for the computational analysis. It should be noted that the current engine is not targeted to passenger cars but rather to medium-duty vehicles such as large vans or even small trucks. The vehicle specifications in Table 2, therefore, correspond to the largest LD vans available in the European market belonging to category $N_1$ Class III.

## 4. Results and discussion

### *4.1. Vehicle and engine results during a typical driving cycle*

Employing the methodology described in the previous section, Fig. 3 demonstrates second-by-second engine and vehicle performance and emission results during one of the studied driving cycles, in this case the WLTC; the results obtained are fully compatible with those obtained from purely experimental approaches on the test bench (e.g. Bielaczyc et al., 2015; Marotta et al., 2015; Dimaratos et al., 2016). During the urban part of the WLTC (0–1022 s), corresponding to phases low and medium in Fig. 1 (GTR No. 15, 2014), where the vehicle speeds are maintained at low to medium levels, the rolling resistance force $F_r$ prevails over the aerodynamic one. During motorway driving, on the other hand, the aerodynamic force assumes much higher values supported by the large vehicle frontal area and the much smaller dependence of rolling resistance on vehicle speed (Giakoumis and Zachiotis, 2017).

In general, the lower the engaged gear (this results in high gear ratio $i_g$ in Table 2), e.g. during the urban parts of the cycle, the smaller the total vehicle moment of inertia, ultimately leading to higher acceleration values and

emissions in Fig. 3 (Rakopoulos and Giakoumis, 2009). On the other hand, the higher the engaged gear (hence the lower the respective gear ratio), the higher the vehicle speed and the lower the accelerations in the cycle owing to now greater vehicle inertia (Gillespie, 1992).

The development of the engine speed in Fig. 3 is largely patterned after the vehicle acceleration. The development of both power and fueling (torque too) follows a similar profile throughout the cycle, as all these engine properties are inter-related with engine loading. During the urban segments of the cycle, the engine loading is mainly determined by the vehicle acceleration. This is due to the fact that during these parts, the absolute vehicle speeds are low but the transient events both frequent and steep resulting in increased inertia terms. During the highway segments, on the other hand, where the vehicle acceleration values are small, it is the increased vehicle speed that mostly influences the engine loading through the aerodynamic resistance force contribution (Gillespie, 1992); the loading then determines the values for torque, power and fuel consumption. Unsurprisingly, at each acceleration in the cycle, fueling peaks at high values owing to the power needed to overcome the vehicle inertia and the various losses in the transmission system.

Further to the above, the points where the most abrupt accelerations are experienced lead also to a considerable overshoot in emissions. It is well known that net soot production (fueling and $CO_2$ emissions as well) is mainly dependent on engine load (Heywood, 1988). With increasing load, e.g. during each acceleration in the cycle, more fuel is injected into the cylinders, increasing the temperatures in the fuel-rich zones; at the same time, the duration of diffusion combustion is prolonged favoring soot formation. On the other hand, two prominent soot oxidation contributors, namely the availability of oxygen and the remaining time after combustion, decrease; thus, the production of soot is favored (Heywood, 1988). During the accelerations in the cycle, the above mechanism is enhanced by the locally very high values of fuel–air ratios experienced during turbocharger lag. For the overshoot in soot emissions observed in Fig. 3 at each acceleration, the main cause is the instantaneous lack of air due to turbocharger lag, further aided by the initial

sharp increase in ignition delay during the early transient cycles of each individual transient event (Rakopoulos and Giakoumis, 2009).

For NO emissions, the main parameter is the burned gas temperatures. Locally high temperatures, due to close to stoichiometric air–fuel mixtures, increase NO emissions during the turbocharger lag thermodynamic cycles. This is due to the fact that for the production of NO there are two contributing parameters, namely high temperatures *and* oxygen availability (Heywood, 1988). During the turbocharger lag phase at the onset of each acceleration in the cycle, soot peaks owing to lower than stoichiometric conditions. During these phases however, and as long as lambda is lower than unity, the availability of air is limited, hence the overshoot in NO emissions is not that pronounced (Rakopoulos and Giakoumis, 2009). Lastly, following basic combustion principles, the $CO_2$ overshoots in Fig. 3 are patterned exactly after the fueling ones.

### *4.2. Comparison of the eight driving cycles*

It is pointed out that the comparison between the eight cycles performed in this section aims to identify *vehicle speed profile effects only*, and not differences located in the individual testing procedure. In order to perform this kind of comparison, it is assumed in the next paragraphs that all driving schedules are examined over the same ‘conditions’, e.g. vehicle test mass, ambient temperature, gear-shift strategy. By doing so, we eliminate all test-procedure-related differences and isolate the vehicle speed-profile effects. This was also the case in other comparative analyses, such as for example in Steven (2013) and Sileghem et al. (2014). Of course, for type approval purposes on the chassis-dynamometer, each test schedule is carried out according to its specific test procedure, as this is outlined in the relevant regulatory documents. Particularly as regards the employed gearshift strategy employed, it was the one discussed in the WLTP documents, i.e. the engine speed based gearshift (Tutuianu et al., 2013).

#### *4.2.1. Vehicle and engine operating envelope*

Figure 4 compares the vehicle speed/acceleration distribution, and Fig. 5 the engine speed/power one for the examined cycles. Intentionally, the x and y axes in all sub-diagrams of Fig. 4 have the same limits (0 to 140 km/h and –4 to 4 m/s$^2$) and equally so for Fig. 5 (1000 to 2600 rpm and 0 to 180 kW), so that the results be easily comparable between the cycles. As argued in the previous section, elevated engine speeds and/or loads originate from either sharp accelerations (urban segments) or high vehicle speeds (motorway driving).

The first, rather obvious, comment has to do with the unique engine operating profile during the highly 'repetitive' NEDC. Here, the individual speed/acceleration tested points (Fig. 4) as well as the engine operating ones (Fig. 5) are the fewest compared to all the other cycles. Notice that even the NYCC and the US06, which have half the duration of the NEDC, exhibit more actual operating points. The explanation lies in the 'repetitiveness' of the NEDC, as the first segment (0–195 s) is repeated four times during the cycle execution, i.e., the first 780 s actually correspond to 195 unique tested points. The prolonged cruising segments of the cycle further reduce the number of actual tested points. The fact that during the motorway part of the NEDC the vehicle assumes speeds up to 120 km/h is responsible for the occurrence of a few engine operating points at rather 'high' speeds and loads in Fig. 5. Of particular mentioning are the very limited values of accelerations during the NEDC, of the order of 1 m/s$^2$ at the maximum (Fig. 4), i.e. 3.6 km/h/s; this means that according to the cycle, at least 27 s are needed to reach 100 km/h from standstill.

Contrary to the modal NEDC, the vehicle and engine operating envelopes of all the other cycles are quite dense and, on occasion, wider/broader too. This holds particularly true for the WLTC 3-2 which encompasses a considerable variety of daily (transient) driving from idling and low-load to highway conditions, and also manifests prolonged duration of 30 min (therefore, 1800 unique operating points). The WLTC exhibits a particularly dense concentration of operating points at low to medium speeds and loads (as does the FTP-75 and the JC08), suggesting a fairly satisfactory coverage of urban driving. The cycle also manifests the highest engine speeds, as these correlate with the vehicle speed. Unarguably, this is the single cycle

with the broadest coverage of the engine operation. The much broader distribution of engine operation during the WLTC over the NEDC confirms the considerable progress in terms of simulated real-world driving behavior, as has also been reported by Steven (2013). For approximately 84% of the time during the WLTC, the vehicle operates in transient conditions (accelerating or decelerating), in contrast to only 37% during the NEDC. Similarly, cruising time is almost absent throughout the WLTC. Overall, 78% of the operating points during the NEDC correspond to lower than 2600 rpm engine speed and 82% to lower than 20 kW power for the tested vehicle in Fig. 5; for the WLTC, the respective numbers are much smaller, 55% and 68%.

The Japanese JC08 exhibits a quite dense distribution in the low to medium speeds and loads region, as the cycle itself clearly focuses on urban/suburban driving. On the other hand, the motorway part is very limited, as Fig. 1 indicates. This is then reflected in rather few operating points at high vehicle speeds (Fig. 4) and engine speeds/loads (Fig. 5).

The results during the U.S. cycles are quite interesting and revealing too. It should be emphasized at first that no U.S. cycle is intended to simulate the widest possible vehicle operation, but rather each cycle ‘enhances’ and complements the other. As a result, the urban/suburban FTP-75 possesses an engine operating profile quite similar to the Japanese JC08; this was also the result reached by Steven (2013). Moreover, these cycles have almost the same maximum speed. Although the FTP-75 has 1877-s duration, the unique operating points in Figs. 4 and 5 are actually 1372, as the first and last 505 s of the cycle produce identical points (see also Fig. 1). A strict acceleration limit of 1.5 m/s$^2$ is evident in Fig. 4; this derives from the fact that at the time the FTP-75 was developed and first put into use (in 1972, initially as FTP-72 without the last 505-s, hot-started segment), the Clayton dynamometers employed were limited to such acceleration values to avoid tire slip (Kruse and Huls, 1973).

The predominantly suburban HFET presents a compact distribution in the low to medium speed and load range too but this is not the result of frequent transient driving (as is the case with the FTP-75 or the JC08). Instead, its profile is primarily derived from prolonged driving at higher than 70 km/h vehicle speeds, with fewer and, more importantly, milder accelerations at high

engaged gears, typical when driving on a motorway (cf. the comments made earlier for Fig. 3). This feature will prove pivotal with regard to emissions during the cycle as will be discussed in the next section. The extra-urban profile of the cycle is best highlighted in Fig. 4 where a lack of low-speed operating points is observed. The obvious absence of penetration in high speeds and loads from the FTP-75 and HFET is remarkably compensated for by the US06; the latter, following its high speeds and harsh accelerations, is the cycle exhibiting the broadest engine speed/load coverage from the eight studied driving schedules (obviously the coverage is not the most dense too, as the US06's duration, at 10 min, is short compared to the other cycles, owing to its use in the U.S. federal legislation as a supplemental driving schedule). Moreover, the US06 is the cycle that manifests the highest demanded power from the vehicle.

The California LA-92, as Fig. 1 confirms, presents a similar driving profile as the FTP-75, but reaching somewhat higher vehicle speeds as well as accelerations in Fig. 4; not surprisingly the engine operating range in Fig. 5 resembles that of the FTP-75.

Lastly, the unique schedule of the NYCC is reflected into the engine operating at predominantly low speeds and loads; however, owing to harsh accelerations, operation at elevated loads/speeds is instantaneously reached at certain points throughout the cycle. Owing to short duration and prolonged idling, the engine operating envelope of the NYCC is rather thin.

One important note that needs to be mentioned here regarding the results of Fig. 5 is that owing to all cycles being 'run' in this study under normal (i.e. fully warmed-up) engine operating conditions, the four identical segments of the NEDC produce the same pairs of power-speed points; the same holds true for the first and last 505-s segments of the FTP-75, as well as for the first and last 300-s segments of the California LA-92. Of course, during real-world test-bench certification, engine power/speed results would be different between cold and hot-started segments.

Figures 6 and 7 expand on the previous graphs by directly comparing the driving and engine activity between the U.S. and European cycles. More specifically, Fig. 6 compares the speed/acceleration distribution of the three U.S. cycles studied in this work that are employed in the federal legislation for

tailpipe emission testing of LD vehicles (FTP-75, HFET, US06) with the NEDC (left sub-diagram), and the WLTC 3-2 (right sub-diagram). It is made quite clear how limited the driving activity during the NEDC is (and how considerably enhanced the driving profile of the U.S. cycles is), and how this huge difference is going to be alleviated with the advent of the WLTC 3-2 in Europe from September 2017; still, operation at harsh accelerations will be absent as the right sub-diagram of Fig. 6 indicates. It should be noted, however, that one element of the thin driving activity representation during the NEDC compared to the U.S. cycles or the WLTC originates in the much higher idling time of the former (23.7%) compared to the latter (11.7% for the three U.S. cycles and 12.6% for the WLTC).

Based on the results presented in Fig. 6, it is not surprising that the engine operating envelope during the three U.S. cycles is vastly broader compared to the modal NEDC (left sub-diagram of Fig. 7), leaving rather wide space for manufacturers in Europe to apply cycle beating techniques (Kadijk et al., 2015; Giakoumis, 2017). Again, the differences are considerably 'smoothed' when the comparison is between the U.S. cycles and the WLTC 3-2 (right sub-diagram of Fig. 7); the latter drive schedule seems to cover almost entirely the operating range of the three U.S. cycles with the exception of some 'extreme' operating points originating in the harsh accelerations of the US06.

It should be pointed out here that the fourth cycle employed for tailpipe emission testing in the United States, namely the SC03, was not included in the analysis, as this cycle is run under specific conditions (35$^{o}$C ambient temperature, air condition on, high sun loading), which cannot be simulated by the present methodology.

*4.2.2. Comparison of emissions, and correlation with cycle metrics*

For the next stage of comparison between the eight cycles, the focus is on emissions, as illustrated in Table 3 and Fig. 8 which demonstrate cumulative emissions of soot, NO, $CO_2$ as well as fuel consumption; these results have been calculated from the methodology presented in Section 3. A characteristic vehicle metric when running on a driving cycle, namely the

energy consumption or demand, is also provided in Table 3 and discussed in the next paragraphs.

From Fig. 8 and Table 3 it becomes evident that urban driving at low speeds with frequent stop-and-go conditions (e.g. the NYCC, FTP-75 and JC08 cycles) results in the biggest amount of emitted pollutants; this holds particularly true for soot. The strong dependence of emitted pollutants on urban driving can be explained from the fact that both average and maximum vehicle accelerations assume higher values during the low-speed (and medium-speed) segments/cycles compared to the high-speed/motorway ones (Watson and Janota, 1982). In this regard, it is not surprising that the 'soft' accelerations throughout the NEDC have resulted in rather low soot emissions, and the same holds true for the motorway-oriented (therefore, less transient) HFET. On the other hand, the extremely harsh NYCC exhibits the highest amount of emitted soot and NO from the examined vehicle.

Further, the low-speed segments are usually characterized by many micro-trips. This means that the percentage of (harsh) accelerations from zero loading is much higher, contributing accordingly to the amount of emitted pollutants. It is reminded here that owing to the turbocharger lag, engine-out emission overshoots from turbocharged diesel engines, such as the one studied here, are more prominent the lower the initial operating conditions (Rakopoulos and Giakoumis, 2009).

On the other hand, the energy demand seems to go along with the $CO_2$ emissions (hence fuel consumption). The latter parameters are all influenced not only by abrupt accelerations but also by prolonged driving at high speeds, hence the NEDC's effects are not negligible here (HFET's too). Notice in Table 3 and Fig. 8 that the results during the Japanese JC08 and the European NEDC are almost identical with regard to fuel and energy consumption; for the former, this originates in the extensive urban segment, whereas for the latter it is the result of prolonged motorway driving. Figure 9, which directly compares the emissions and consumption during the low and the extra-high segment of the WLTC cycle is provided at this point, in order to expand on the latter arguments. Clearly, the milder accelerating profile of the motorway part is reflected into significantly lower emissions, particularly soot which is primarily influenced by abrupt speed and load changes. On the other

hand, both the energy and fuel consumption between the two examined segments assume similar values. Another interesting result drawn from Table 3 is that although considerably more transient (hence possessing a higher energy demand value), the WLTC results in somewhat lower $CO_2$ emissions compared to the NEDC. This was also the result reached by Steven (2013) and Marotta et al. (2015), and can be attributed, at least for the current vehicle, to the slightly higher engine load level during the WLTC compared to the NEDC, which is then reflected into slightly higher engine efficiency.

A well-established cycle metric associated with (engine-out) exhaust emissions, particularly from turbocharged diesel engines, is the number of stops per km, detailed in Table 1 for the examined cycles (Giakoumis, 2017). The lower left sub-diagram of Fig. 10 eloquently demonstrates the association between the emitted cumulative soot from the examined vehicle with the cycles' stops per km; an impressive correlation with $R^2$ equal to 0.997 is established. Equally strong is the correlation between NO and stops/km ($R^2$=0.987) but somewhat weaker between fuel consumption (or $CO_2$) and stops/km ($R^2$=0.86) or energy consumption and stops/km ($R^2$=0.74), as the other sub-diagrams of Fig. 10 indicate. As will be argued later in the text, fuel and energy consumption are influenced not only by abrupt accelerations (urban driving) but by high vehicle speeds too (motorway driving without intermediate stops), hence the weaker correlation with stops/km. In this figure, the exclusively motorway HFET is the driving schedule that differentiates from the others in terms of energy and fuel consumption.

On the other hand, and confirming fully the results by Tu et al. (2013), soot correlated rather weakly with average speed ($R^2$=0.41), and poorly with maximum acceleration ($R^2$=0.06) or accelerations per minute ($R^2$=0.06). Similarly weak or even poor were the correlations between NO or fuel consumption with the above cycle metrics.

The relative positive acceleration (RPA), another well-established metric of the cycle's aggressiveness (Table 1), is on display in Fig. 11 for all the examined cycles. It is reminded that RPA is defined as the integral of the product of instantaneous speed and instantaneous positive acceleration over a defined section of a route or a test cycle.

As is usually the case, RPA decreases with increasing driving speed (the US06 seems to diversify from this trend, as this is a harsh cycle with predominantly high speeds). In Fig. 11, values for both parts of the NEDC, the urban ECE-15 and the extra-urban EUDC are demonstrated.

Regarding soot, its correlation with RPA was found weaker (compared to stops/km), with $R^2$=0.64 (0.73 if the US06 is excluded). On the other hand, NO correlated slightly better with RPA ($R^2$=0.70), and fuel consumption/$CO_2$ even better ($R^2$=0.83). Energy consumption was found to correlate highly with RPA, as the $R^2$ value reached 0.94 in this case; all the above correlations are demonstrated in Fig. 12.

Lastly, both studied pollutants correlated well with energy consumption ($R^2$=0.74 for soot and 0.81 for NO) and this was even more the case for fuel consumption ($R^2$=0.95).

In order to shed more light into the relevant trends, Fig. 13 is provided that illustrates cumulative emission and consumption results for six urban cycles or cycle segments; with reference to Fig. 1, these are the ECE-15 part of the NEDC (4x185 = 780 s), the entire NYCC (600 s), the first 1035 s of the JC08, the stabilization phase (867 s) of the FTP-75, the two city parts of the US06 (t=0–120 s and t=496–600 s), as well as the low-speed part of the WLTC 3-2 (589 s). Excluding the US06-city segment, for all the other drive schedules maximum speed ranges between 45 km/h (NYCC) and 62 km/h (JC08).

In general, and confirming the results of past research, the higher the RPA, the higher the amount of emitted soot, NO, and energy consumption, with the exception of the US06. For the latter cycle, the amount of emitted soot during its city part is 3.3 times higher than the average during the whole cycle (0.132 g/km compared to 0.04; 69% of the soot (in miligrams) emitted during the US06 is actually produced during its city segment), whereas the RPA is 2.3 times higher the entire cycle's. This results in the cycle segment exhibiting particularly high $CO_2$ emissions and energy consumption. What seems initially odd is that the emitted soot during the US06-city is much lower compared to the NYCC, despite the higher RPA value of the former (0.51) compared to the latter (0.35). The explanation lies in the argument raised earlier regarding the dependence of turbocharged diesel engines emitted soot on abrupt accelerations from low speeds/loads, best identified through the

stops/km cycle metric; there are 7.90 stops per km during the NYCC compared to ‘only’ 1.75 for the US06-city.

## 5. Summary and conclusions

A detailed fundamental analysis of eight driving schedules was performed with respect to their technical attributes, and effects on engine-out emissions and fuel consumption from a turbocharged diesel-powered large van. To this aim, a comprehensive vehicle model was coupled to a mean-value emissions sub-model experimentally calibrated at transient conditions such as the ones experienced during a driving cycle. The schedules examined ranged from purely urban (NYCC) to whole driving pattern cycles (NEDC, JC08, WLTC, FTP-74, LA-92), up to purely highway (HFET) or even ‘extreme’ cases (US06).

Predictably, vehicle speed was identified as the dominant property affecting almost all vehicle parameters, and performance in general. A significant differentiation was observed between urban and motorway segments in this respect. As regards the engine, it was the rotational speed fluctuations (initiated by the respective vehicle accelerations) that influenced decisively the engine performance and emissions. At each point in the cycle where an (abrupt) increase in the vehicle speed was experienced, an overshoot in engine-out emissions (particularly soot) was noticed too; the culprit here was the turbocharger lag.

From the comparison of the eight driving schedules, the 1800-s duration worldwide WLTC 3-2 was identified as the cycle with a very broad and, at the same time, quite dense coverage of vehicle and engine performance. This was, by far, the single cycle with the fullest coverage of the typical daily vehicle activity. The supplemental US06 exhibited even broader distribution, owing to some particularly harsh accelerations involved. The Japanese JC08 as well as the U.S. FTP-75 and California LA-92 were characterized by a somewhat similarly-shaped envelope of engine operating conditions in terms of speed and power. This clearly focused on low to medium speeds/loads, owing to the predominantly urban/suburban profile of these cycles. On the other hand, the only modal, and also ‘repetitive’, cycle in this investigation, the European NEDC, manifested a considerably thin coverage of engine and

vehicle operation, being thus highly unrepresentative of real driving activity, particularly when compared to its U.S. counterparts. Lastly, the exclusively suburban/highway U.S. HFET and the urban NYCC, owing to their simulation of specific (and even extreme for the case of the NYCC) driving activity, manifested rather narrow coverage of the engine speed/power operation. For the case of the HFET this included the medium speed/power range, and for the NYCC the low-medium one.

Regarding the engine-out emitted pollutants, and confirming the results of previous research, it was found that the individual attributes of each cycle and its specific driving profile obviously influenced the emitted pollutants and $CO_2$. More specifically, the more transient cycles (or cycle segments) were more polluting too, exhibiting also higher energy consumption values. Urban driving at low speeds with frequent stop-and-go conditions (e.g. the NYCC, FTP-75 and JC08 cycles) was responsible for the biggest contribution in emissions in g/km. This was particularly true for soot, which is primarily influenced by abrupt accelerations. Stops/km as well as RPA were found to correlate well with soot and NO, fueling and energy consumption. In contrast, average speed, maximum acceleration as well as accelerations/min could not be correlated with any exhaust emission. During urban driving, the emitted pollutants peaked in contrast to the quasi-steady-state highway segments. On the other hand, fuel consumption and energy demand assumed comparable values during both urban (owing to abrupt and frequent accelerations) and extra-urban (owing to elevated vehicle speeds) segments.

Although driving cycles have been employed for many decades for the certification of new vehicles, and will continue to do so, it is rather safe to assume that no (legislated) cycle will ever fully cover the whole engine/vehicle operating range. That is why real driving emissions (RDE) tests are gaining increased attention in the legislation as, for example, the one to be implemented during the EU certification of new passenger cars. The current study, not being associated with sophisticated and costly drive cycle measurement procedures, can offer important advantages, as a limitless number of different driving schedules can be run in a matter of a few seconds. These schedules can then be evaluated from the point of view of both cycle metrics and vehicle emissions, taking into account the very critical emission

pattern during transients. Another important aspect is that due to the analysis being carried out on a *second-by-second basis* (instead of the 'cumulative' approach followed during drive cycles' emissions measurements), the particular instances of the driving schedule can be highlighted that mostly contribute to the emitted pollutants and $CO_2$. It is this interaction between *instantaneous* cycle properties and exhaust emissions provided by the current methodology as well as the strong correlations established between stops/km and emitted pollutants, and between RPA and fuel/energy consumption, that can facilitate the construction, assessment and implementation of new driving schedules. Lastly, the current computational procedure can also prove effective surrogate tool for real-world driving emissions, as parameters such as road inclination, road traffic etc can be easily incorporated in the input driving schedule file, and their influence be evaluated immediately.

## References

André, M., Joumard, R., Hickmam, A.J., Hassel, D., 1994. Actual car use and operating conditions as emission parameters: derived urban driving cycles. Science Total Environ. 146/147, 225–233.

Austin, T.C., diGenova, F.J., Carlson, T.R., Joy, R.W., Gianolini, K.A., Lee, J.M., 1993. Characterization of driving patterns and emissions from light-duty vehicles in California. California Air Resources Board, Final report.

Benajes, J., Lujan, J.M., Bermudez, V. and Serrano, J.R., 2002. Modelling of turbocharged diesel engines in transient operation. part 1: insight into the relevant physical phenomena. Proc. IMechE, Part D, J. Automobile Eng. 216, 431–441.

Berg, W., 2003. Legislation for the reduction of exhaust gas emissions, 2003. In: Gruden, D., (Editor), The Handbook of Environmental Chemistry, Vol. 3, Traffic and Environment, Springer-Verlag, Berlin, pp. 175–253.

Berglund, S., 1993. A model of turbocharged engines as dynamic drivetrain members. SAE Paper No. 933050.

Bielaczyc, P., Woodburn, J., Szczotka, A., 2015. A comparison of carbon dioxide exhaust emissions and fuel consumption for vehicles tested over the NEDC, FTP-75 and WLTC chassis dynamometer test cycles. SAE Paper No. 2015-01-1065.

Bishop, J.D.K., Stettler M.E.J., Molden, N., Boies, A.M., 2016. Engine maps of fuel use and emissions from transient driving cycles. Appl. Energy 183, 202–217.

Degobert, P., 1995. Automobiles and Pollution. Editions Technip, Paris.

Dimaratos A., Tsokolis, D., Fontaras, D., Tsiakmakis, S., Ciuffo B., Samaras, Z., 2016. Comparative evaluation of the effect of various technologies on light-duty vehicle $CO_2$ emissions over NEDC and WLTP. Transport. Res. Procedia 14, 3169–3178.

Ericson, C., Westerberg, B., Egnell, R., 2005. Transient Emission Predictions with Quasi Stationary Models. SAE Paper No. 2005-01-3852.

Filipi, Z., Wang, Y., Assanis, D., 2001. Effect of variable geometry turbine (VGT) on diesel engine and vehicle system transient response. SAE Paper No. 2001-01-1247.

Gambarotta, A., Lucchetti, G., Vaja, I., 2001. Real-time modelling of transient operation of turbocharged diesel engine. Proc. Inst. Mech. Eng., Part D: J. Automobile Eng. 225, 1186–1203.

Giakoumis, E.G., 2017. Driving and Engine Cycles. Springer, Cham, Switzerland.

Giakoumis, E.G., Alafouzos, A.I., 2010. Study of diesel engine performance and emissions during a transient cycle applying an engine mapping-based methodology. Appl. Energy 87, 1358-1365.

Giakoumis, E.G., Lioutas, S.C., 2010. Diesel-engined vehicle nitric oxide and soot emissions during the European light-duty driving cycle using a transient mapping approach. Transport. Res. Pt. D: Transp. Environ. 15, 134–143.

Giakoumis, E.G., Zachiotis, A.T., 2017. Investigation of a diesel-engined vehicle's performance and emissions during the WLTC driving cycle - Comparison with the NEDC. Energies 10, doi:10.3390/en10020240.

Gillespie, T.D., 1992. Fundamentals of Vehicle Dynamics. SAE International, Warrendale, PA.

Global Technical Regulation No. 15, 2004. Worldwide harmonized light vehicles test procedure. Established in the Global Registry on 12 March 2014.

Heywood, J.B., 1988. Internal Combustion Engine Fundamentals. McGraw-Hill, New York.

Jiang, Q., Van Gerpen, J.H., 1992. Prediction of diesel engine particulate emission during transient cycles. SAE Paper No. 920466.

Joumard, R., André, M., Vidon, R., Tassel, P., Pruvost, C., 2000. Influence of driving cycles on unit emissions from passenger cars. Atmos. Environ. 34, 4621–4628.

Kadijk, G., van Mensch, P., Spreen, J., 2015. Detailed investigations and real-world emission performance of Euro 6 diesel passenger cars. TNO Report 2015 R10702.

Kruse, R.E., Huls, T.A., 1973. Development of the federal urban driving schedule. SAE Paper No. 730553.

Kruse RE, Paulsell CD., 1974. Development of a highway driving cycle for fuel economy measurements. EPA.

Marotta, A., Pavlovic, J., Ciuffo, B., Serra, S., Fontaras, G., 2015. Gaseous emissions from light-duty vehicles: moving from NEDC to the new WLTP test procedure. Environ. Sci. Technol. 49, 8315–8322.

Pelkmans, L., Debal, P., 2006. Comparison of on-road emissions with emissions measured on chassis dynamometer test cycles. Transport. Res. Pt. D: Transp. Environ. 11, 233–241.

Rackmil, C.I., Blumberg, P.N., Becker, D.A., Schuller, R.R., Garvey, D.C., 1988. A dynamic model of a locomotive diesel engine and electrohydraulic governor. ASME Trans., J. Engineering Gas Turbines Power 110, 405–414.

Rakopoulos, C.D., Giakoumis, E.G., 2009. Diesel Engine Transient Operation. Springer, London.

Sileghem, L., Bosteels, D., May, J., Favre, C., Verhelst, S., 2014. Analysis of vehicle emission measurements on the new WLTC, the NEDC and the CADC. Transport. Res. Pt. D: Transp. Environ. 32, 70−85.

Steven, H., 2013. Homologation test cycles worldwide-Status of the WLTP. Green Global NCAP labelling / Green scoring Workshop.

TransportPolicy.net. http://www.transportpolicy.net/index.php?title=Category:Light-duty_Vehicles. Accessed 12 March 2016.

Tu, J., Wayne, W.S., Perchinschi, M.G., 2013. Correlation analysis of duty cycle effects on exhaust emissions and fuel economy. J Transport Res. Forum 52, 97–115.

Tutuianu, M., Marotta, A., Steven, H., Ericsson, E., Haniu, T., Ichikawa, N. et al., 2013. Development of a world-wide harmonized light duty driving test cycle (WLTC). UN/ECE/WP.29/GRPE/WLTP-IG Technical Report, DHC Group.

Tzirakis, E., Pitsas, K., Zannikos, F., Stournas, S., 2006. Vehicle emissions and driving cycles: Comparision of the Athens driving cycle (ADC) with ECE-15 and European driving cycle (EDC). Global NEST Journal 8, 282–90.

U.S. Environmental Protection Agency, 1993. Federal test procedure review project preliminary technical report, U.S.EPA 420-R-93-007.

Watson, N., Janota, M.S., 1982. Turbocharging the Internal Combustion Engine. McMillan, London.

Winterbone, D.E., Benson, R.S., Mortimer, A.G., Kenyon, P., Stotter, A., 1977. Transient response of turbocharged diesel engines. SAE Paper No. 770122.

Zhou, M., Jin, H., 2017. Development of a transient fuel consumption model. Transport. Res. Pt. D: Transp. Environ. 51, 82–93.

## Figure Captions

**Fig. 1.** Vehicle speed profile of the eight examined driving cycles (all are transient except for the modal NEDC)

**Fig. 2.** Flowchart demonstrating the computational procedure

**Fig. 3.** Engine and vehicle performance and emission results during the WLTC Class 3-2 cycle for the engine/vehicle under study ($F_r$ corresponds to the rolling resistance force and $F_{total}$ to the sum of rolling and aerodynamic resistance); vertical dashed lines designate the limits of each segment of the cycle

**Fig. 4.** Vehicle speed/acceleration distribution of the eight examined driving schedules (notice the modal character of the NEDC, the strict ±1.5 $m/s^2$ acceleration limits of the FTP-75, the exclusively highway profile of the HFET, the extreme accelerations of the US06, the narrow range of the JC08, and the dense pattern of the WLTC)

**Fig. 5.** Engine speed/power operating range throughout the eight examined driving schedules for the engine/vehicle under test (dashed line in each sub-diagram corresponds to the engine's full-load power)

**Fig. 6.** Comparison of the engine speed/acceleration distribution between the three U.S. cycles and the NEDC (left sub-diagram) or the WLTC 3-2 (right sub-diagram); total idling time for the three U.S. cycles is 11.7% compared to 23.7% for the NEDC and 12.6% for the WLTC

**Fig. 7.** Comparison of the engine speed/power operating range between the U.S. cycles and the NEDC (left sub-diagram) or the WLTC 3-2 (right sub-diagram) for the engine/vehicle under investigation

**Fig. 8.** Cumulative emitted soot and NO, $CO_2$, fuel consumption and energy consumption throughout the eight examined driving schedules for the engine/vehicle under study

**Fig. 9.** Comparison of cumulative emitted NO and soot, $CO_2$, fuel consumption, energy consumption and RPA throughout the low and the extra-high segment of the WLTC 3-2 for the engine/vehicle under study

**Fig. 10.** Correlation between soot, NO, fuel consumption and energy consumption with stops/km for the engine/vehicle under study running on the eight examined driving schedules (the maximum values correspond to the NYCC; the cycle with zero stops/km is the exclusively motorway HFET)

**Fig. 11.** Relative positive acceleration with respect to vehicle driving speed (i.e. excluding idling) for the eight examined driving cycles

**Fig. 12.** Correlation between soot, NO, fuel consumption and energy consumption with RPA for the engine/vehicle under study running on the eight examined driving schedules (the values at the maximum RPA correspond to the NYCC)

**Fig. 13.** Cumulative emitted NO and soot, $CO_2$, fuel consumption, energy consumption and RPA throughout six urban driving segments/cycles for the engine/vehicle under study (see text for exact definition of stabilization phase and urban/city segments)

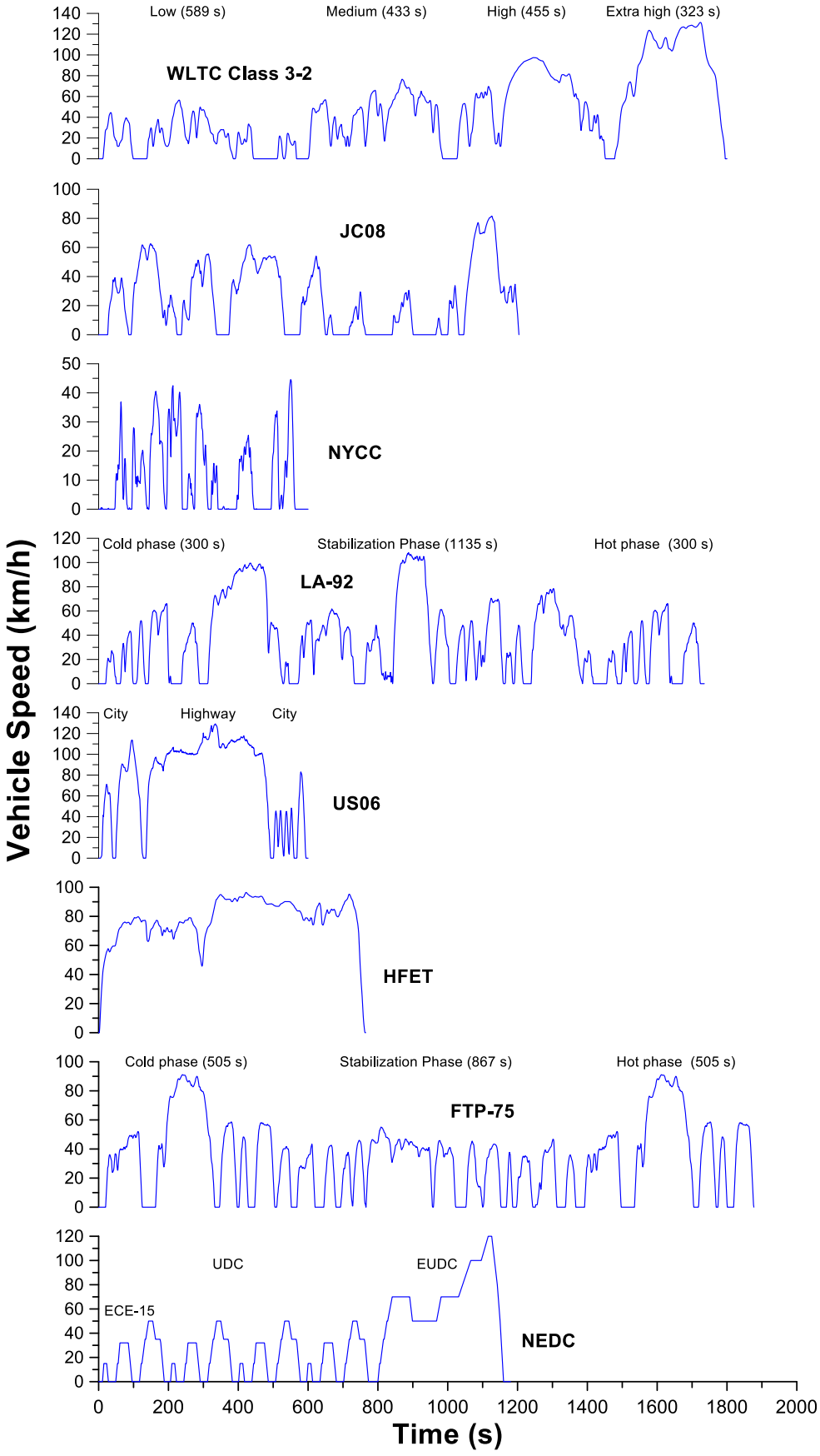


**Fig. 1.** Vehicle speed profile of the eight examined driving cycles (all are transient except for the modal NEDC)

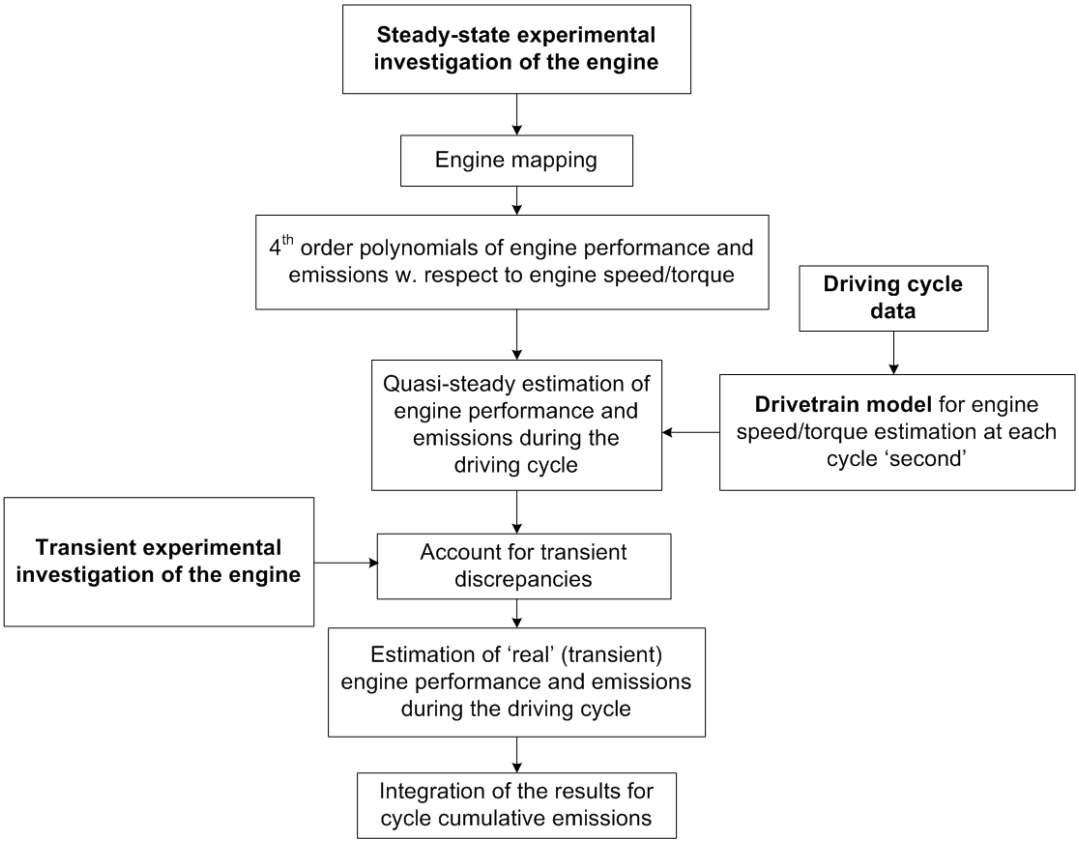


**Fig. 2.** Flowchart demonstrating the simulation-experimental procedure

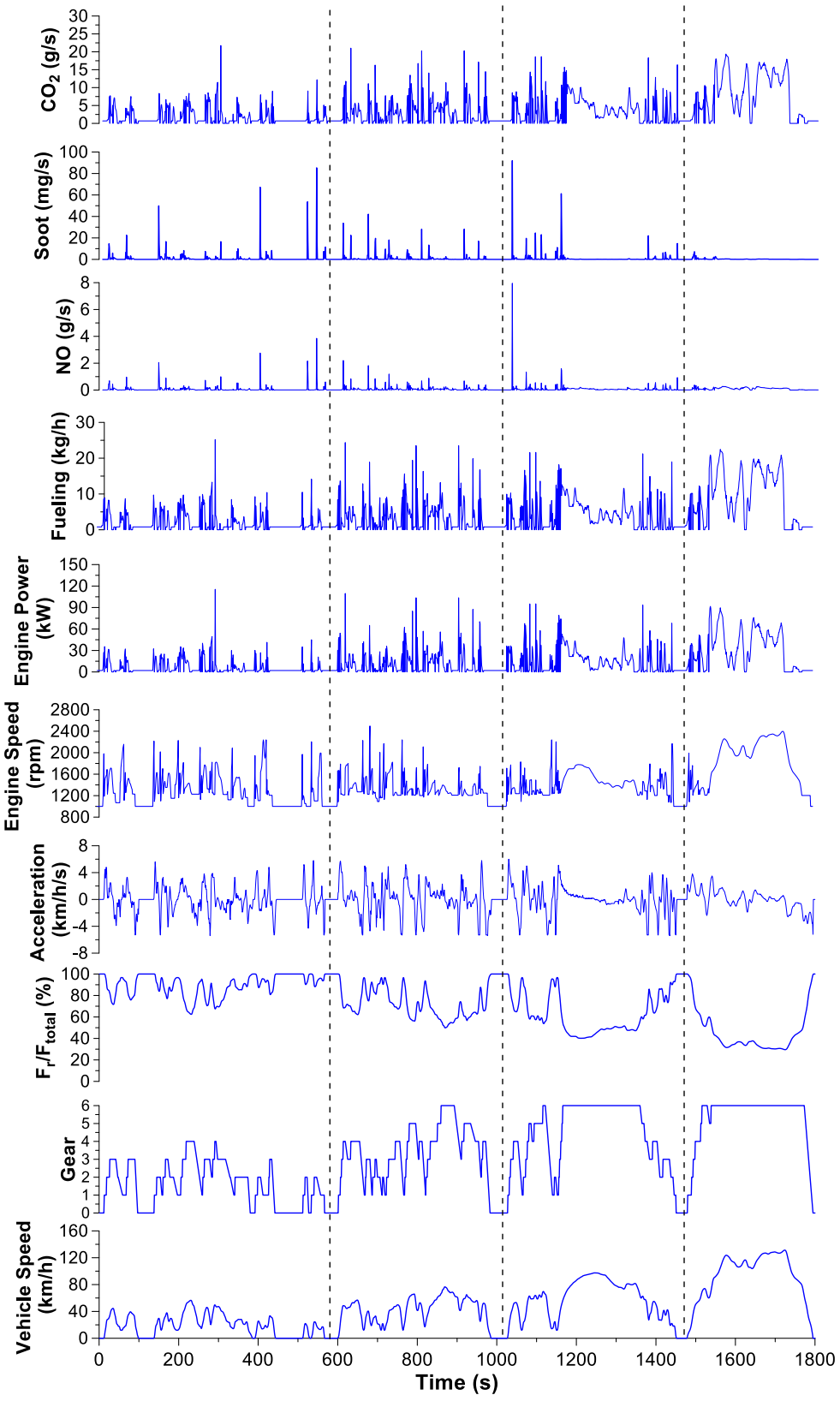


**Fig. 3.** Engine and vehicle performance and emission results during the WLTC Class 3-2 cycle for the engine/vehicle under study ($F_r$ corresponds to the rolling resistance force and $F_{total}$ to the sum of rolling and aerodynamic resistance); vertical dashed lines designate the limits of each segment of the cycle

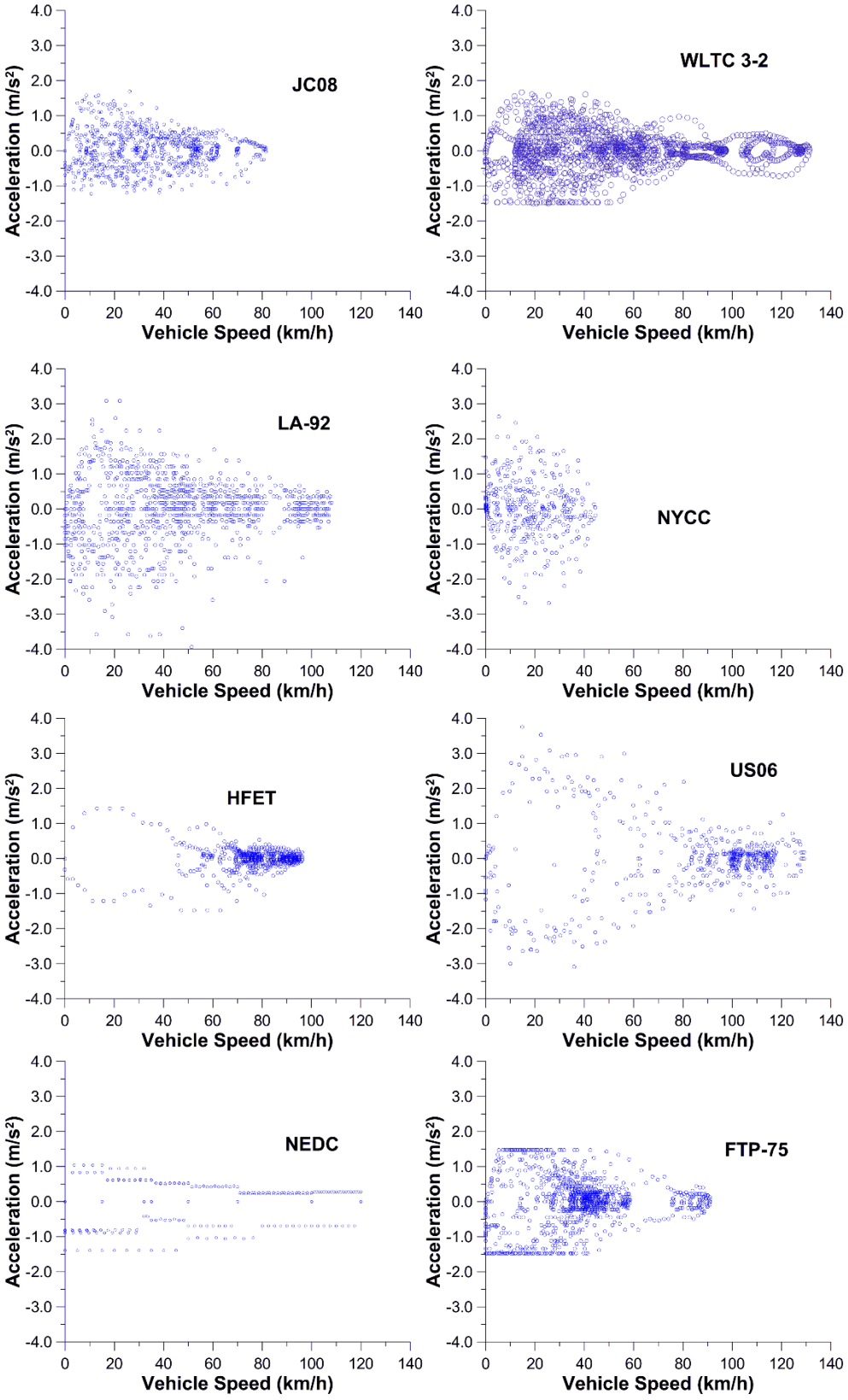


**Fig. 4.** Vehicle speed/acceleration distribution of the eight examined driving schedules (notice the modal character of the NEDC, the strict ±1.5 m/s$^2$ acceleration limits of the FTP-75, the exclusively highway profile of the HFET, the extreme accelerations of the US06, the narrow range of the JC08, and the dense pattern of the WLTC)

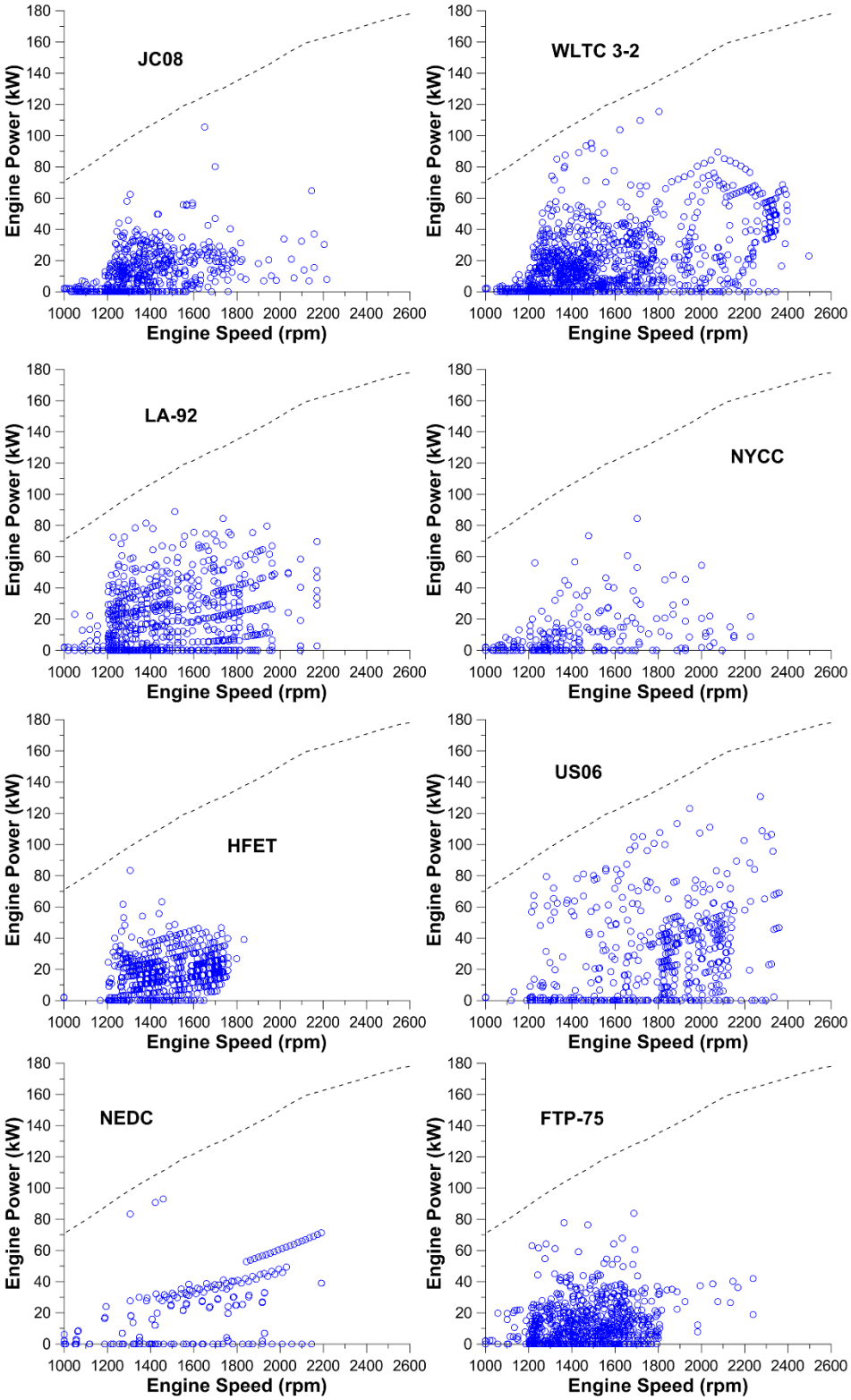


**Fig. 5.** Engine speed/power operating range throughout the eight examined driving schedules for the engine/vehicle under test (dashed line in each sub-diagram corresponds to the engine's full-load power)

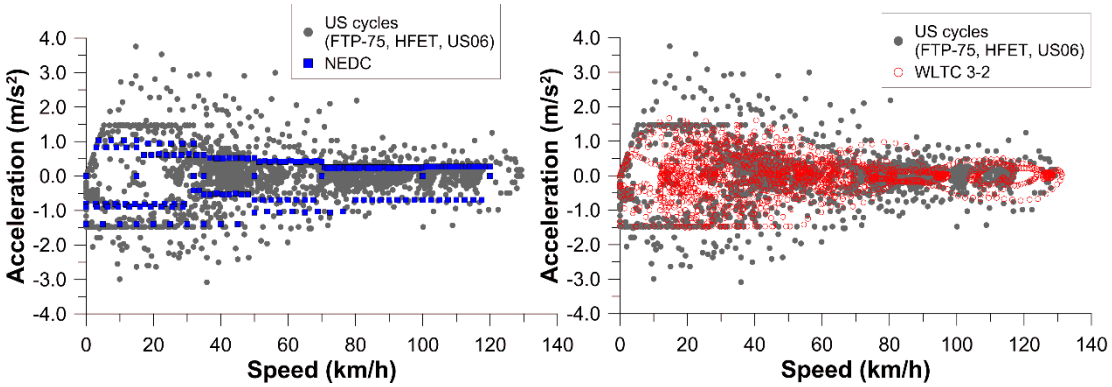


**Fig. 6.** Comparison of the engine speed/acceleration distribution between the three U.S. cycles and the NEDC (left sub-diagram), or the WLTC 3-2 (right sub-diagram); total idling time for the three U.S. cycles is 11.7% compared to 23.7% for the NEDC and 12.6% for the WLTC

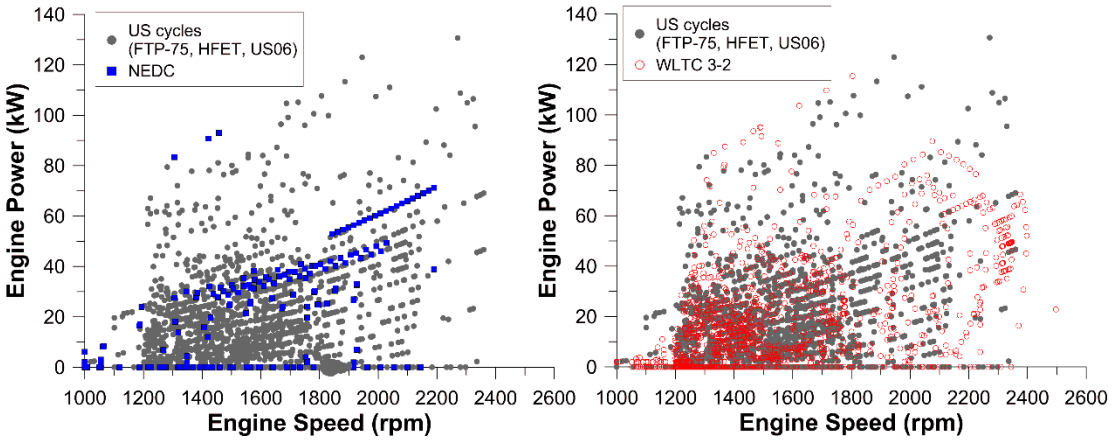


**Fig. 7.** Comparison of the engine speed/power operating range between the U.S. cycles and the NEDC (left sub-diagram), or the WLTC 3-2 (right sub-diagram) for the engine/vehicle under investigation

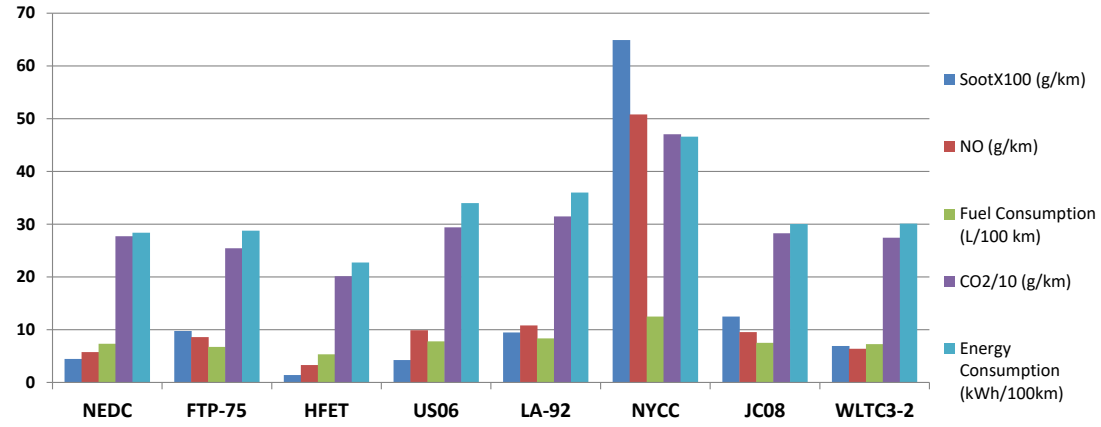


**Fig. 8.** Cumulative emitted soot and NO, $CO_2$, fuel consumption and energy consumption throughout the eight examined driving schedules for the engine/vehicle under study

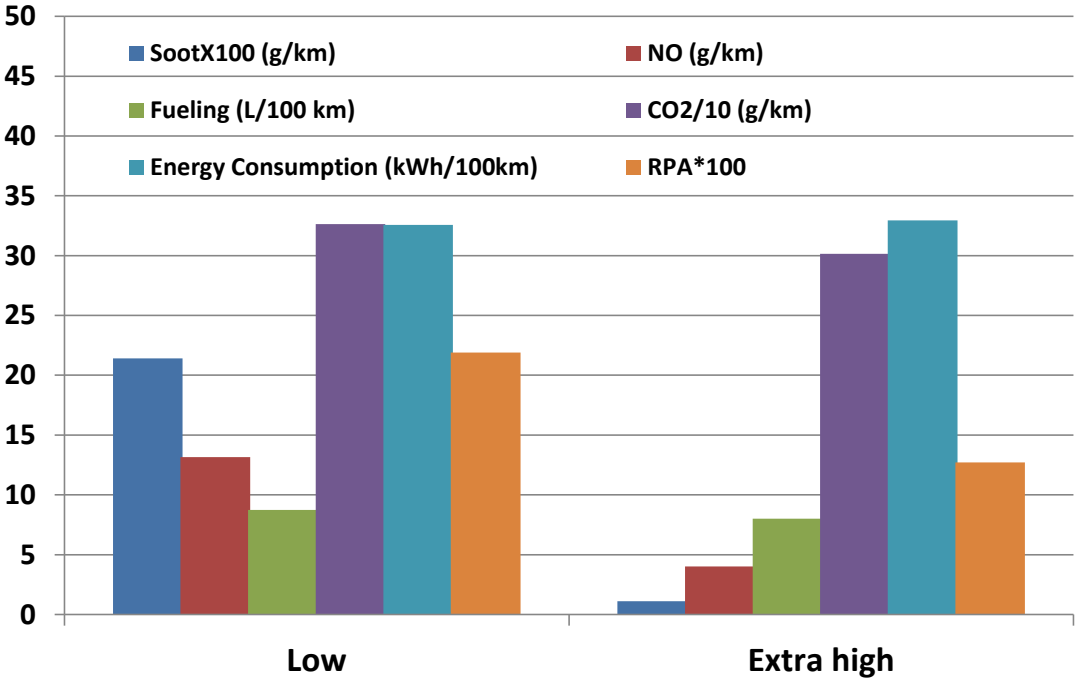


**Fig. 9.** Comparison of cumulative emitted NO and soot, $CO_2$, fuel consumption, energy consumption and RPA throughout the low and the extra-high segment of the WLTC 3-2 for the engine/vehicle under study

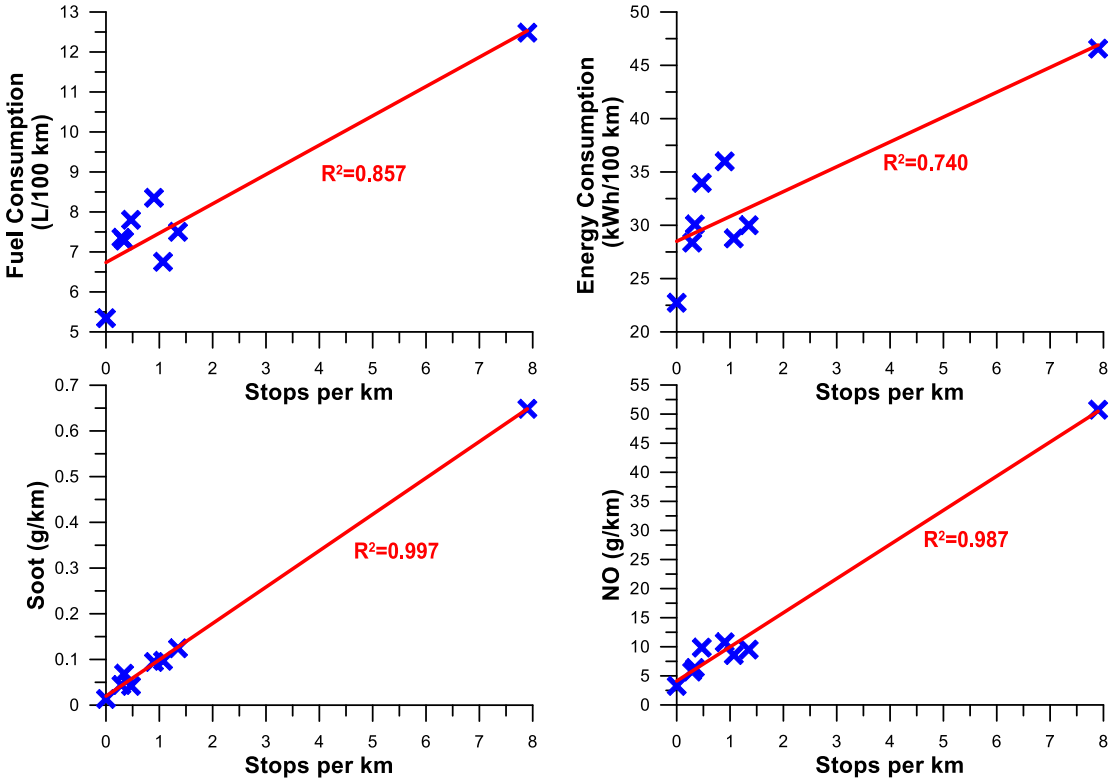


**Fig. 10.** Correlation between soot, NO, fuel consumption and energy consumption with stops/km for the engine/vehicle under study running on the eight examined driving schedules (the maximum values correspond to the NYCC; the cycle with zero stops/km is the exclusively motorway HFET)

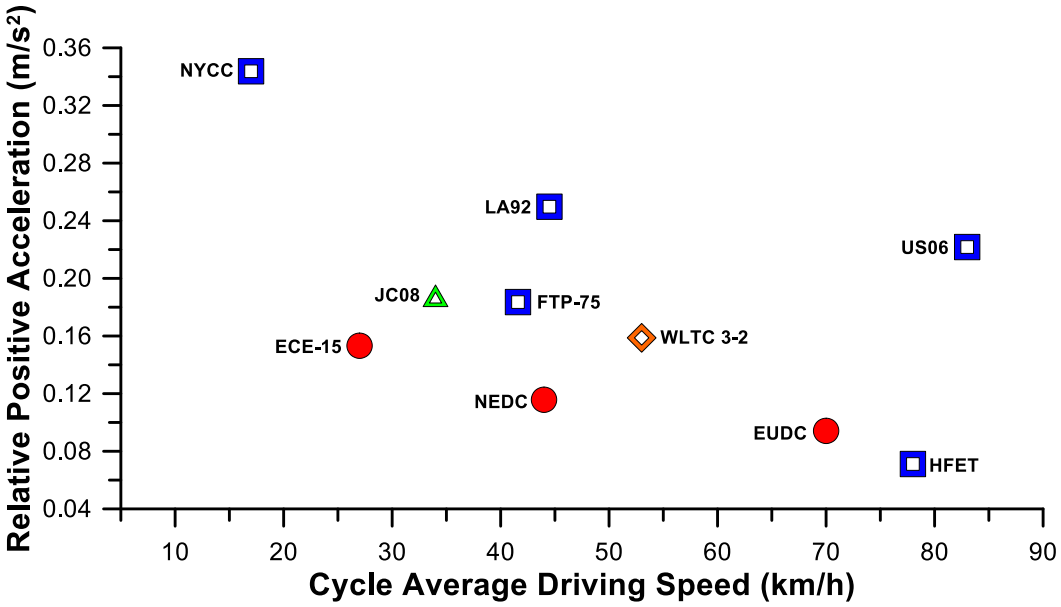


**Fig. 11.** Relative positive acceleration with respect to vehicle driving speed (i.e. excluding idling) for the eight examined driving cycles

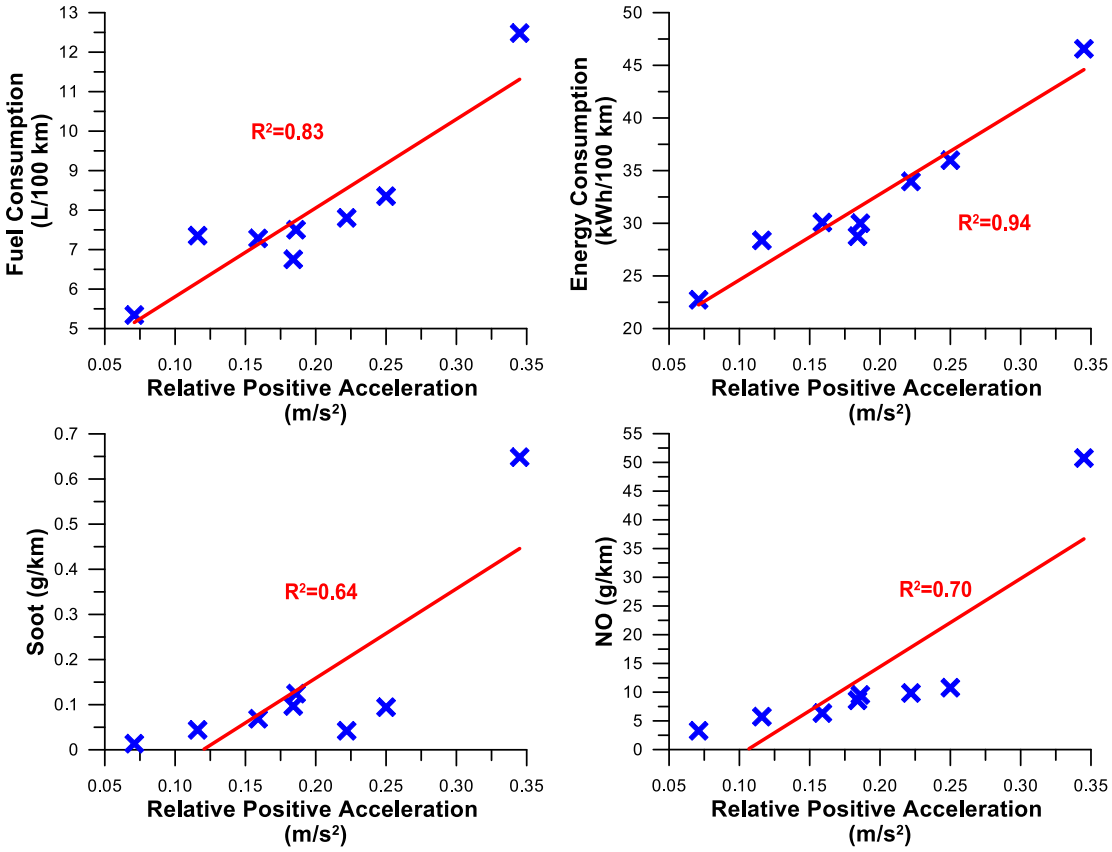


**Fig. 12.** Correlation between soot, NO, fuel consumption and energy consumption with RPA for the engine/vehicle under study running on the eight examined driving schedules (the values at the maximum RPA correspond to the NYCC)

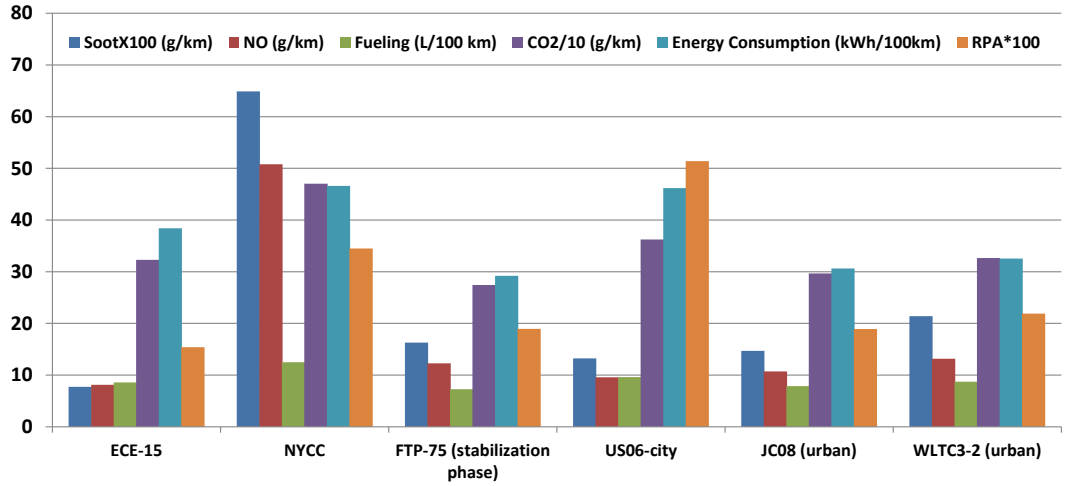


**Fig. 13.** Cumulative emitted NO and soot, $CO_2$, fuel consumption, energy consumption and RPA throughout six urban driving segments/cycles for the engine/vehicle under study (see text for exact definition of stabilization phase and urban/city segments)

**Table 1.** Summary of main technical specifications of the eight examined driving cycles

| Cycle | Duration (s) | Distance (km) | Max. Speed (km/h) | Average Speed (km/h) | Max. Accel. ($m/s^2$) | Idling Time (%) | RPA ($m/s^2$) | Accels per min. | Stops per km |
|---|---|---|---|---|---|---|---|---|---|
| **NEDC** | 1180 | 11.000 | 120.0 | 33.6 | 1.04 | 23.7 | 0.116 | 1.58 | 0.29 |
| **FTP-75** | 1877 | 17.769 | 91.2 | 34.1 | 1.48 | 18.0 | 0.184 | 2.49 | 1.07 |
| **HFET** | 765 | 16.507 | 96.4 | 77.7 | 1.43 | 0.50 | 0.071 | 2.04 | 0 |
| **US06** | 600 | 12.888 | 129.2 | 77.3 | 3.76 | 6.5 | 0.222 | 3.40 | 0.47 |
| **LA-92** | 1735 | 17.706 | 108.1 | 36.7 | 3.08 | 17.5 | 0.250 | 2.87 | 0.90 |
| **NYCC** | 600 | 1898 | 44.6 | 11.4 | 2.68 | 32.2 | 0.345 | 2.70 | 7.90 |
| **JC08** | 1204 | 8159 | 81.6 | 24.4 | 1.69 | 28.7 | 0.186 | 2.29 | 1.35 |
| **WLTC 3-2** | 1800 | 23.266 | 131.2 | 46.5 | 1.67 | 12.6 | 0.159 | 2.27 | 0.34 |

**Table 2.** Data of the engine and vehicle used for the analysis

| | |
|---|---|
| **Engine** | |
| **Engine type** | Four-stroke, in-line, six-cylinder, turbocharged, aftercooled, direct-injection diesel engine |
| **Bore / Stroke** | 97.5 mm / 133 mm |
| **Compression ratio** | 18:1 |
| **Maximum power** | 177 kW @ 2600 rpm |
| **Moment of inertia** | 0.87 kg $m^2$ |
| **Vehicle** | |
| **Gross Vehicle Weight** | 3.5 tn |
| **Frontal area** | 3 $m^2$ |
| **Aerodynamic resistance coefficient** | 0.38 |
| **Gear ratios** | 5.78; 2.7; 1.9; 1.25; 1.0; 0.9 |

**Table 3.** Comparison of the cumulative engine-out emissions, and fuel and energy consumption for the eight driving cycles

| Cycle | Energy Demand (kWh/100 km) | Soot (g/km) | NO (g/km) | Fuel Consumption (L/100 km) | $CO_2$ (g/km) |
|---|---|---|---|---|---|
| **NEDC** | 28.40 | 0.0447 | 5.778 | 7.36 | 277.15 |
| **FTP-75** | 28.79 | 0.0976 | 8.618 | 6.76 | 254.44 |
| **HFET** | 22.76 | 0.0141 | 3.318 | 5.35 | 201.38 |
| **US06** | 34.00 | 0.0427 | 9.900 | 7.81 | 293.96 |
| **LA-92** | 36.02 | 0.095 | 10.820 | 8.36 | 314.69 |
| **NYCC** | 46.59 | 0.649 | 50.80 | 12.49 | 470.40 |
| **JC08** | 30.03 | 0.125 | 9.563 | 7.51 | 282.91 |
| **WLTC 3-2** | 30.10 | 0.0694 | 6.403 | 7.29 | 274.57 |